Journal Pre-proof

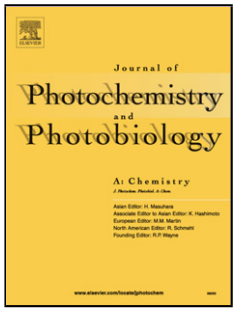

Synthesis, photophysical and DFT studies of naphthyl chalcone and nicotinonitrile derivatives

Hemant Hegde, Rajeev K. Sinha, Suresh D. Kulkarni, Nitinkumar S. Shetty

PII: S1010-6030(19)31333-4

DOI: https://doi.org/10.1016/j.jphotochem.2019.112222

Reference: JPC 112222

To appear in: *Journal of Photochemistry & Photobiology, A: Chemistry*

Received Date: 5 August 2019

Revised Date: 2 November 2019

Accepted Date: 5 November 2019

Please cite this article as: Hegde H, Sinha RK, Kulkarni SD, Shetty NS, Synthesis, photophysical and DFT studies of naphthyl chalcone and nicotinonitrile derivatives, *Journal of Photochemistry and amp; Photobiology, A: Chemistry* (2019), doi: https://doi.org/10.1016/j.jphotochem.2019.112222

Synthesis, photophysical and DFT studies of naphthyl chalcone and nicotinonitrile derivatives

Hemant Hegde[a], Rajeev K. Sinha[b], Suresh D. Kulkarni[b] and Nitinkumar S. Shetty[a*]

[a] *Department of Chemistry, Manipal Institute of Technology, Manipal Academy of Higher Education, Manipal, Karnataka, India-576104.*

[b] *Department of Atomic and Molecular Physics, Manipal Academy of Higher Education, Manipal, Karnataka, India-576104.*

[*]nitin.shetty@manipal.edu

Graphical abstract

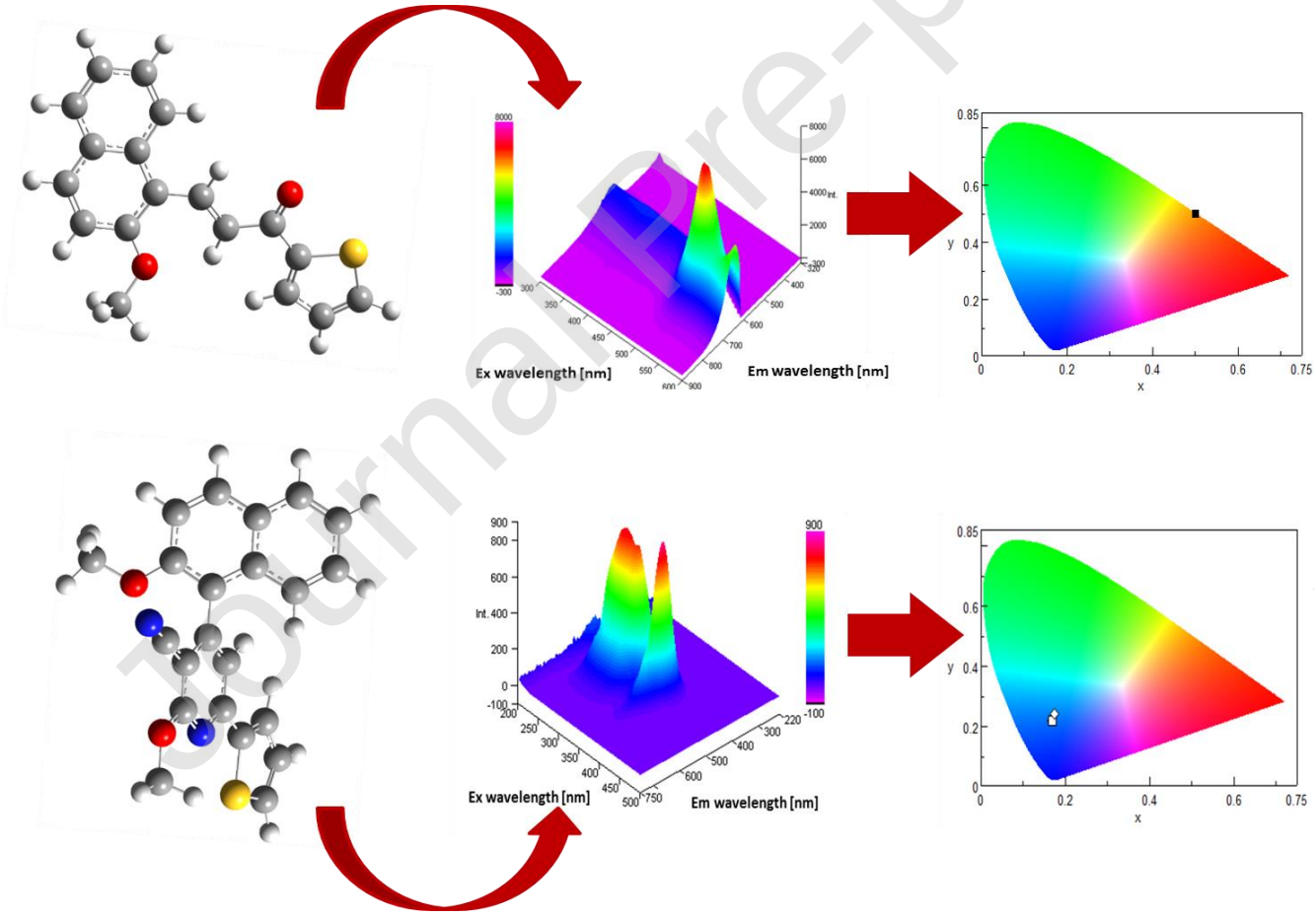

Highlights:

- Synthesis & characterization of naphthyl chalcone and cyanopyridine are reported
- Absorption & emission properties calculated by density functional theory
- Orbital picture of all excitations were identified as π->π*
- Cyanopyridine emits blue & green while naphthyl chalcone showed orange emission
- Naphthyl chalcone showed orange emission in solid-state & well-suited for OLEDs

Abstract:

Chalcone and cyanopyridine derivatives have emerged as attractive light sensitive materials, with potential use in cell probing and optoelectronic applications. They are highly fluorescent both in solution and solid state and thus well-suited for OLED applications. Herein, we report the synthesis of a chalcone derivative (**CP1**) using the Claisen Schmidt condensation of 2-acetyl thiophene and 2-methoxy naphthaldehyde followed by the heterocyclization to yield the novel cyanopyridine derivative (**NP1**). Synthesized molecules were characterized using elemental analysis, FTIR and NMR spectra. Density functional theory (DFT) calculations were performed on the molecules, in order to understand their absorption and emission properties. The orbital picture of all the excitations involved in these transitions were identified as π->π*. The, experimentally obtained FTIR spectra were in excellent agreement with DFT calculated infrared spectrum. The steady state fluorescence spectra of CP1 showed dual emission in the blue and green regions while a single band, orange emission was observed for the other molecule NC1. NC1 showed the solid-state emission in orange region inferring its suitability for the OLED application.

Keywords: Chalcone, cyanopyridine, DFT, fluorescence.

1. Introduction

Besides being suitable for promising biological activities such as anticancer, antimicrobial, antidepressant, immunosuppressive, anti-inflammatory, etc. [1-7], chalcone and its derivatives have displayed numerous other properties like optical [8], photochemical [9, 10] and NLO properties, and have been used as fluorescent dyes, in light emitting diodes, fluorescent sensors and as fluorescent probes [11].

As a member of the π-conjugated system, the optical properties of chalcone and its derivatives, have received considerable attention owing to its nonlinear optical and fluorescence property, due to the delocalization of electronic charge and overlapping π orbitals. Furthermore, as a family of traditional luminogenic materials, chalcone and its derivatives often possess strong emissions in the solution state, but their luminescence gets quenched at high-concentrations or/and solid states [12, 13]. However, their optical properties are easily controlled by introducing electron donor or acceptor groups to aromatic rings. Fluorescence of chalcones have been utilized for many applications such as cell probe in a mouse embryonic stem cell [14]. Therefore, the fluorescent study of chalcones has been area of interest in photochemistry.

In view of the considerable importance and adjustable structure of chalcone and its derivatives, designing and synthesizing a chalcone that can emit strong fluorescence in solid state is possible. On the other hand, heterocyclisation of chalcone derivative has produced worthwhile compounds with widespread applications. Therefore, several reports are available for the synthesis of nicotinonitrile (cyanopyridines) via chalcones, which produces highly substituted cyanopyridine derivatives [15-21]. Owing to the recent development in the field of organic based optoelectronic materials, study of photophysical properties of diverse organic frameworks has become a major interest in the field of organic chemistry [22, 23].

Cyanopyridines were first reported for their optoelectronic properties by Ahipa *et al.* [24]. The fluorescence spectra of cyanopyridine derivatives were studied both in solution and in liquid crystalline film state. The compounds were found to exhibit good quantum yields (ϕ_f = 28–49 %) in the solution state and satisfactory quantum yields (ϕ_f = 10–22 %) in the film state also. These results support the optoelectronic properties of 2-(4, 6-disubstituted aryl-3-cyanopyridyl) oxy acetohydrazones and also, as an active photo-responsive and electron-transporting material for device applications.

Later, Ershov *et al.* [25] reported 5- or/and 6- aryl substituted cyanopyridine derivative found to possess a solid-state emission with various intensities. The fluorescent maxima of the studied cyanopyridine was found to be in blue region of the spectrum (410-535 nm). Therefore, the cyanopyridine derivatives reported to show high fluorescence intensity which is a basic need of modern light sensitive materials [26]. In agreement with the reported data, the target molecules are designed to possess significant optoelectronic behavior in the solution phase as well as in solid state. This would help in the development of new cyanopyridine derivatives for OLED applications.

Being inspired by the photochemical applications of chalcones and pyridine derivatives, in the present work, we are reporting the synthesis of chalcone derivatives from naphthaldehyde and new nicotinonitrile derivative from there on. The synthesis is followed by (i) structural characterization using Nuclear Magnetic Resonance (NMR), Fourier Transform Infrared (FTIR) spectroscopy and Density Functional Theory (DFT) calculations and (ii) investigation of emissive property using Fluorescence spectroscopy.

2. Material and methods:

2.1 Synthesis of molecular systems

Required chemicals were procured commercially and were used as such without further purification. Thin layer chromatographic technique (TLC) was used to monitor progress of the reaction. Pre-coated aluminum sheets (alichrosep) silica gel-60/UV_{254} was used as stationary phase with I_2 and UV light as visualizing agents. Melting point was checked using Thiele's tube in open capillary tube and was uncorrected. IR spectra were taken on Shimadzu Infrared spectrometer-8400s using KBr as background in pellet form. ^{1}H and ^{13}C NMR spectra were recorded on Bruker NMR-400 MHz and 100 MHz respectively using TMS as an internal standard. Elemental analysis was performed by using Perkin Elmer 2400 CHN elemental analyzer.

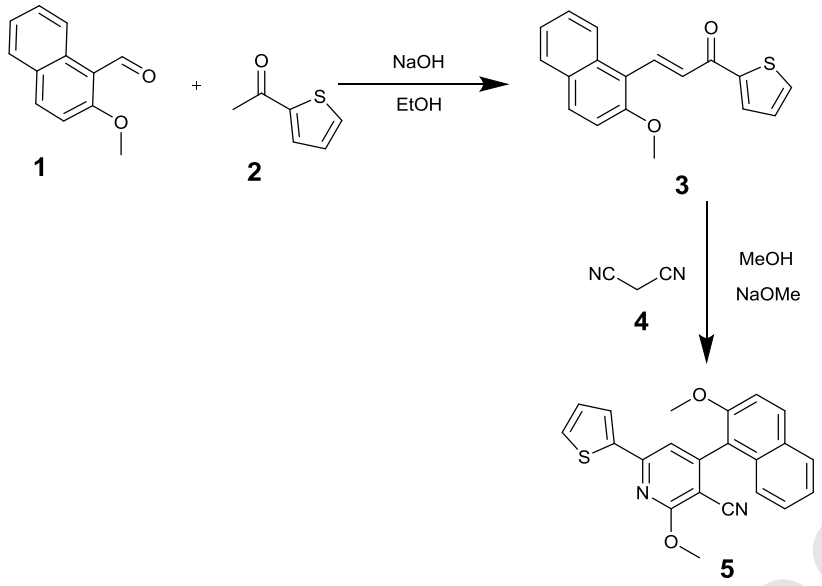

Scheme 1: **Synthesis of 2-methoxy-4-(2-methoxynaphthalen-1-yl)-6-(thiophen-2-yl) nicotinonitrile, 5.**

Synthesis of chalcone derivatives (NC1), 3:

Chalcone derivative of 2-methoxy-1-naphthaldehyde and 2-acetyl thiophene was prepared as earlier reported procedure [27]. The method begins with the generation of enolate ion, by dissolving 2-acetyl thiophene (2.52 g, 20 mmol) in minimum quantity of sodium hydroxide solutions (30 %). To the above solution, 2-methoxy-1-naphthaldehyde (3.72 g, 20 mmol) dissolved in ethanol (2 mL) was added and the reaction mixture was stirred at room temperature to obtain a homogeneous mixture. Stirring was continued at room temperature for 16-18 h. On completion of the reaction (checked by thin layer chromatography), reaction mixture was then poured into the beaker containing crushed ice and neutralized using dil. HCl. Precipitate formed was then filtered and washed with distilled water.

3-(2-methoxynaphthalen-1-yl)-1-(thiophen-2-yl)prop-2-en-1-one (NC1), 3:

Greenish yellow amorphous solid; yield, 5.42 g (92.4 %); m.p.: 122-124 °C; IR spectrum (Fig. S1 in ESI) (γ-max, cm^{-1}): 3080 (Ar-H), 2933 (C-H), 1631 (C=O), 1593(C=C), 1575; ^{1}H NMR (Fig. S2 in ESI) (400 MHz, DMSO-d_6) δ: 8.14-8.15(d, 1H,), 8.07-8.09 (d, 1H, J= 8 Hz, thiophene-H), 8.19-8.21(d, 1H, J= 8 Hz, thiophene-H), 7.91-7.96 (m, 4H, Ar-H), 7.87, 7.61-7.63 (d, 1H, J= 8 Hz, Ar-H), 7.56-7.59, 7.43-7.46 (dd, J= 4 Hz, 2 Hz) 7.30-7.32 (d, 1H, J= 8 Hz, Ar-H), 4.07 (s, 3H, OCH_3) ppm; ^{13}C NMR (Fig. S3 in ESI) (100 MHz, DMSO-d_6) δ: 56.2, 113.8, 118.9, 123.9, 124.0, 127.1, 128.6, 128.68, 129.0,

130.2, 131.7, 133.3, 135.2, 135.4, 145.2, 153.8, 184.0 ppm; Elemental analysis: calctd. for $C_{18}H_{14}O_2S$; C, 73.44; H, 4.79. Found: C, 73.48; H, 4.83.

Synthesis of cyanopyridine derivatives (CP1), 5:

Compound **3** (2.94 g, 10 mmol) was dissolved in 5 mL of methanol and 2.5 mL of sodium methoxide (0.54 g, 10 mmol) solution in methanol was added with constant stirring and the reaction mixture was stirred for 8-9 h at room temperature. The precipitate was filtered and washed with methanol and dried to afford Creamy yellow colored product. The crude product was recrystallised using ethyl acetate.

2-methoxy-4-(2-methoxynaphthalen-1-yl)-6-(thiophen-2-yl)nicotinonitrile (CP1), 5:

Creamy yellow crystalline solid; yield, 3.25 g (87.5 %); m. p.: 234-235 °C; IR spectrum (Fig. S4 in ESI) (γ-max, cm^{-1}): 3090 (Ar-H), 2945 (C-H), 2220 (CN), 1624 (C=N), 1610 (C=C); ^{1}H NMR (Fig. S5 in ESI) (400MHz, DMSO-d_6) δ: 8.16-8.18 (d, 1H, J= 8 Hz, thiophene-H), 7.84-8.04 (m, 5H, Ar-H), 7.65-7.67 (d, 1H, J= 8 Hz, Ar-H), 7.46-7.49 (dd, 2H, J= 4 Hz, Ar-H), 7.42-7.44 (d, 1H, J= 8 Hz, Ar-H) 7.20-7.22 (d, 1H, J= 8 Hz, Ar-H), 4.1 (s, 3H, OCH_3), 3.91(s, 3H, OCH_3) ppm; ^{13}C NMR (Fig. S6 in ESI) (100 MHz, DMSO-d_6) δ: 54.9, 56.9, 95.4, 114.1, 114.7, 115.3, 118.5, 123.9, 124.4, 128.1, 128.3, 128.8, 129.1, 129.5, 131.5, 131.9, 143.0, 153.4, 153.6, 154.0, 164.3 ppm; Elemental analysis: calctd. for $C_{22}H_{16}N_2O_2S$; C, 70.95; H, 4.33; N, 7.52. Found: C, 70.91; H, 4.36; N, 7.57.

2.2 FTIR and fluorescence spectral analysis

FTIR spectral studies were done for the functional group identification of the titled compounds. Samples were prepared by mixing 1:10 synthetic compound and KBr. The mixture was ground to fine powder and pressed to pellets using hydraulic press. Fluorescence spectra were recorded at room temperature using Jasco FP8300 Fluorescence spectrophotometer with 450 W xenon lamp. The compounds were dissolved in acetonitrile to make 0.1 mM, 0.2 mM, 1.0 mM and 10.0 mM solutions.

2.3 Density Functional Theory (DFT) calculations

Density functional theory (DFT) calculations were performed on the molecules of interest in the ground state using Becke-3-Lee-Yang-Parr (B3LYP) theory and Gaussian type basis set 6-311++G(d,p). For the excited state calculations, time dependent (TD) B3LYP method was used. The Ground state geometry optimization was followed by harmonic frequency calculation to ensure the structure to be in

global minimum of the potential energy surface. The UV-Visible spectrum was calculated utilizing vertical excitation from the ground state optimized geometry. The emission spectrum was calculated as adiabatic energy difference between the first excited state and the ground state. All calculations were performed with GAMESS (US) program package [28].

3. Results and discussion

In this work, targeted molecule **5** was synthesized by the reaction between 3-(2-methoxynaphthalen-1-yl)-1-(thiophen-2-yl)prop-2-en-1-one (NC1), **3** and malononitrile in the presence of sodium methoxide as base catalyst [19, 20]. Chalcone was synthesized as precursor molecules by using conventional Claisen Schmidt condensation using 2-methoxy-1-naphthaldehyde and 2-acetyl thiophene in presence of NaOH at room temperature [27].

IR and NMR spectroscopic analysis confirmed the chemical structure of desired products. FTIR spectrum of compound **3** showed characteristic peaks for C=O and C=C of chalcone at around 1631 cm^{-1} and 1593 cm^{-1} respectively. We can observe the absence of these peaks in the cyanopyridine (CP1) **5,** which clearly shows the cyclisation of chalcone to form the corresponding cyanopyridine derivative. The FTIR spectrum of the compound **5** also showed a peak at 2220 cm^{-1} corresponding to -CN group of pyridine which is also evident from ^{13}C NMR spectrum as it showed characteristic signal at δ 95.4 ppm.

3.1 Structural study (FTIR and DFT):

Figure 1(a) and (b) shows the structure of molecules NC1 and CP1 respectively in the ground electronic state, calculated with B3LYP/6-311++G(d,p) level of theory. As it can be seen in the Figure 1(a), in the molecule NC1, the naphthalene and thiophene rings are nearly coplanar. The thiophene ring is bent relative to the naphthalene ring by ~16.9 degrees. In the molecule CP1, shown in Figure 1(b), the pyridine and thiophene aromatic rings are coplanar whereas the plane of pyridine and thiophene rings is bent relative to the naphthalene ring by 109.4 degrees. The xyz coordinates of the optimized structure of NC1 and CP1 molecules are provided in the supplementary Table S1 and S2.

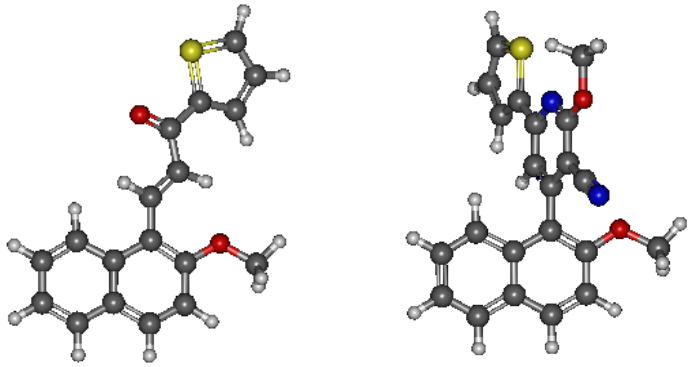

(a) NC1 (b) CP1

Figure 1: Ground state optimized structure of molecules NC1 and CP1 calculated with B3LYP/6-311++G(d,p) level of theory.

FTIR spectrum of molecules NC1 and CP1 are shown in Figure 2(a) and (c) respectively. The spectral position of bands observed in the FTIR spectrum for NC1 and CP1 are shown in supplementary Figure S1 and S4 respectively. The calculated structures of the both NC1 and CP1 are ascertained with the calculated harmonic infrared frequencies shown in Figure 2(b) and (d) respectively. The calculated infrared spectra are scaled with a factor of 0.956. As it is evident from the Figure 2, the calculated spectra are in excellent agreement with the FTIR spectra of two molecules both in terms of position and intensity.

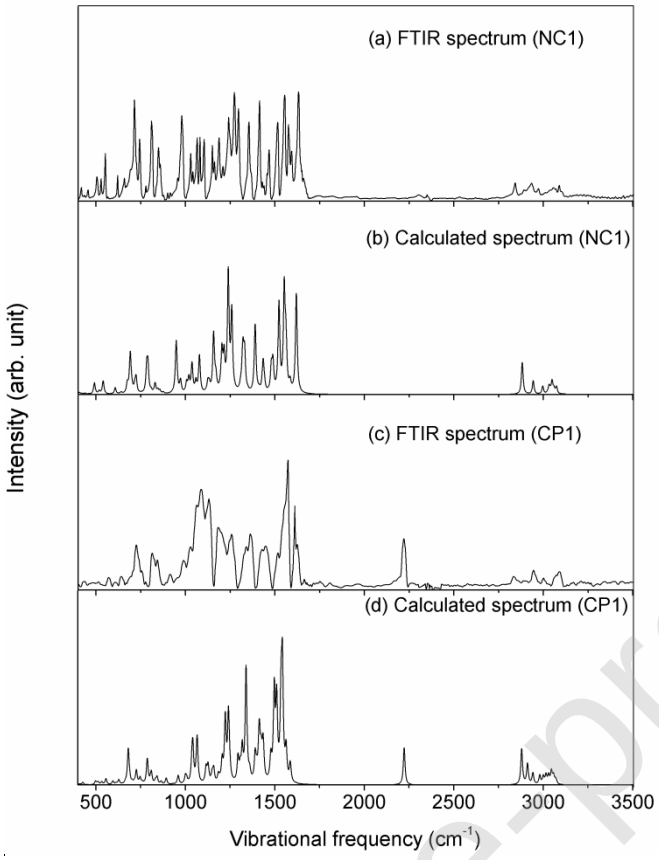

Figure 2: (a) FTIR spectrum of NC1 (b) calculated infrared spectrum of NC1 (c) FTIR spectrum of CP1 and (d) Calculated infrared spectrum of CP1. The calculated spectra were obtained with B3LYP/6-311++G(d,p) theory level. The calculated harmonic frequencies are scaled with a factor of 0.956.

3.2 Fluorescence spectroscopic study

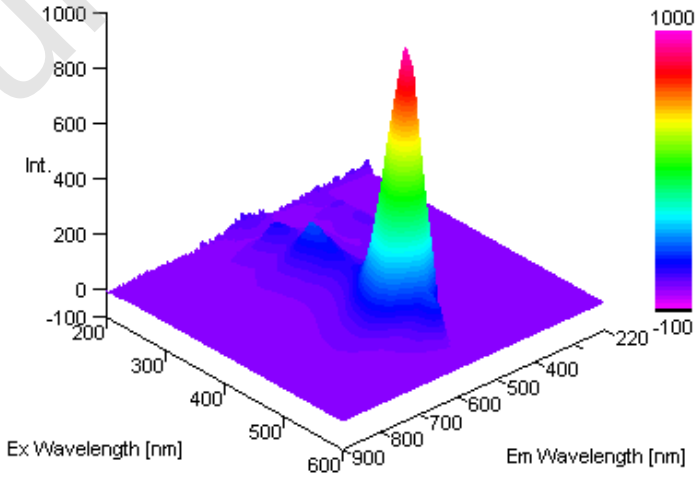

Fig. 3: Fluorescence excitation emission matrix of 0.1 mM NC1.

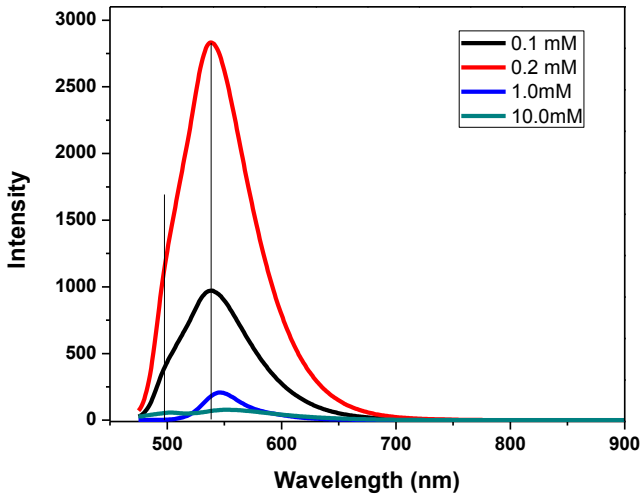

Fig. 4: Fluorescence spectra of NC1 at different concentrations (Excitation wavelength-470 nm)

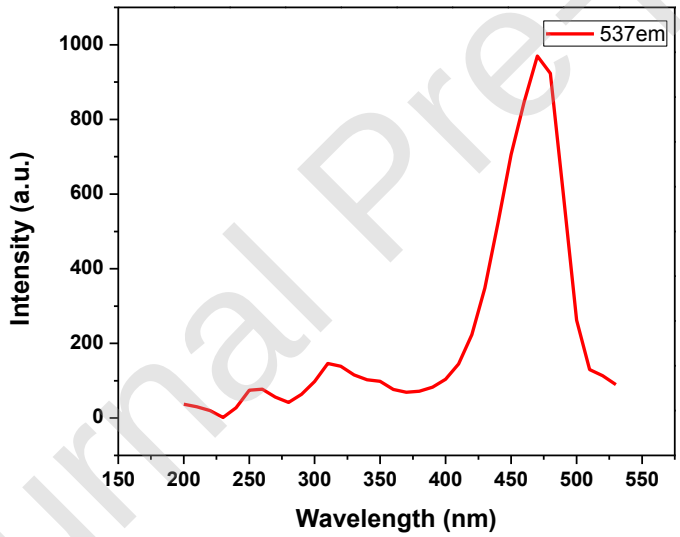

Fig. 5: Excitation spectra of NC1 (emission wavelength-537 nm)

The excitation and emission matrix for NC1 (**Fig. 3**) showed predominantly one emission centered around 537 nm. The fluorescence spectra of NC1 (**Fig. 4**) showed an emission band which is slightly asymmetric. The corresponding excitation spectrum is shown in **Fig. 5**. The intensity was maximum for 0.2 mM concentration and gradually the FWHM of the peak reduced with intensity. The shoulder, poorly visible at lower concentrations was clearly distinguishable at 494 nm at higher (10.0 mM) concentration.

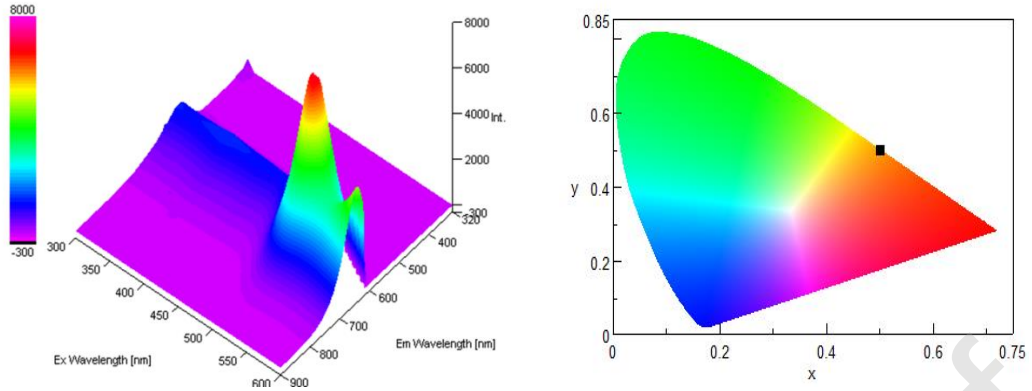

(A) **(B)**

Fig. 6: A) Excitation-emission matrix B) CIE coordinates of NC1 in the Solid-state

The solid-state emission of NC1 is shown in **Fig. 6a**. The excitation emission matrix shows that the emission of NC1 is centered around ~570 nm which has excitation band situated at ~500 nm. The corresponding CIE (Commission Internationale de l'Elcairage) colour coordinates (**Fig. 6b**) shows that the materials emit strongly in the orange region. The solid-state emission can be useful in solid-state lighting applications as the material can be easily excited with visible light.

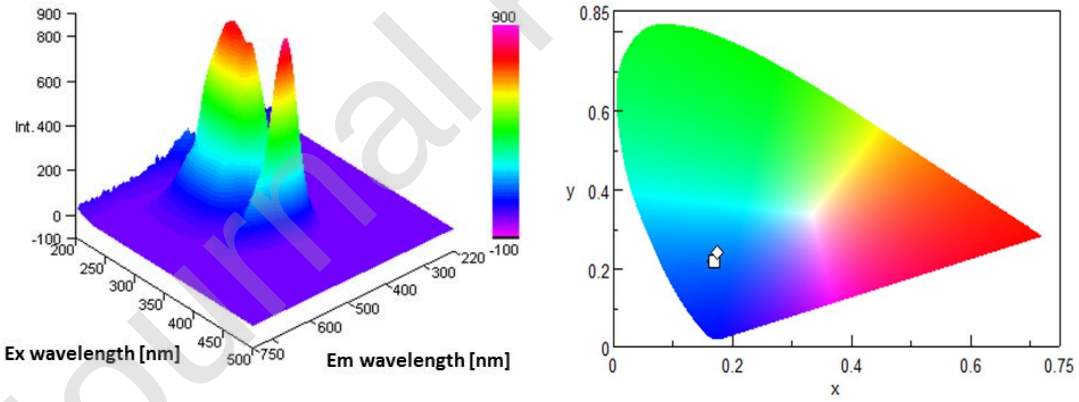

(A) **(B)**

Fig. 7: A) Fluorescence excitation emission matrix B) CIE coordinates of 0.1 mM CP1

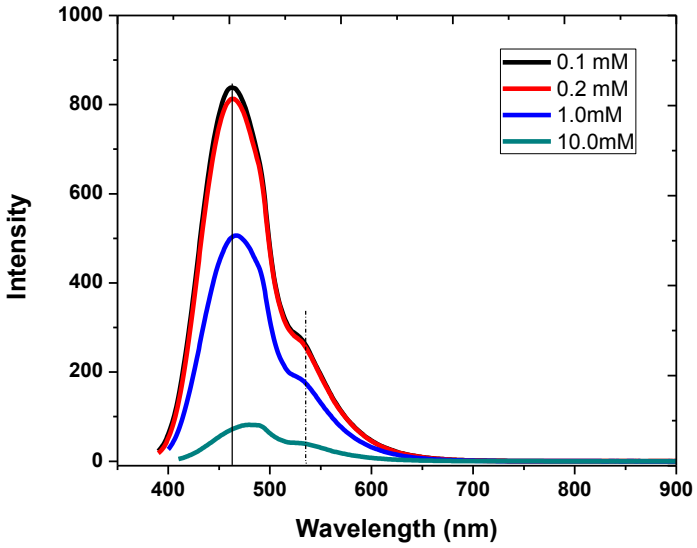

Fig. 8: Fluorescence spectra of CP1 at different concentrations (Excitation wavelength-370 nm)

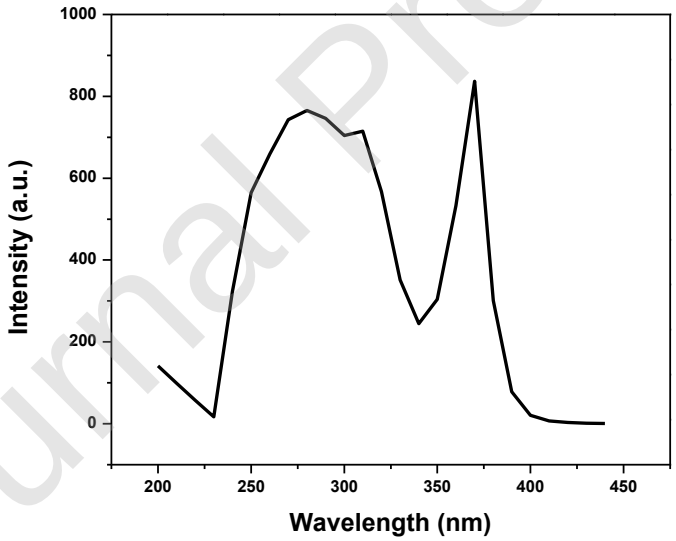

Fig. 9: Excitation spectra of CP1 0.1mM (Emission wavelength-460 nm)

The excitation emission matrix of CP1 (**Fig. 7a**) shows the presence of two excitation bands for the same emission. The corresponding CIE colour coordinates (**Fig. 7b**) show that the material exhibits strong blue emission under UV excitation. The fluorescence spectra of CP1 (**Fig. 8**) showed that the main emission band is centered around 460 nm while the other emission band is a weak shoulder

around 530 nm. Increase in concentration of CP1 led to decreased fluorescence intensity due to concentration quenching [29]. The excitation spectra (**Fig. 9**) revealed that the excitation band in the 230 nm - 340 nm was intense only for 0.1 mM and gradually vanished with increasing CP1 concentration. However, the excitation band at 370 nm was observed for all concentrations though their intensity reduced at higher CP1 concentration.

3.3 Excited state calculations

In order to understand the absorption and emission properties of synthesized molecules NC1 and CP1, excited state density functional theory calculations were performed using time-dependent (TD) B3LYP method. Figure 10 (a) and (b) shows the structure of NC1 and CP1 respectively, in their lowest excited electronic state. The optimized xyz coordinates of two molecules are given in the supplementary Table S3 and S4. Remarkable structural change is observed for NC1 compared to its ground state structure (shown in Figure 1(a)). As it has been discussed earlier, in the ground state, the naphthalene and thiophene ring in the molecule NC1 are nearly planar which changes dramatically in the first excited state. The plane of thiophene ring has changed its orientation and is nearly perpendicular to the naphthalene ring. The angle between two ring planes are 113.96 degrees compared to 16.9 degrees in the ground state. Structural changes were also observed in the molecule CP1. In this molecule, the angle between naphthalene ring and pyridine ring is 96.6 degree compared to 109.4 degree in the ground state. The pyridine and thiophene rings are coplanar as it was observed in the ground state.

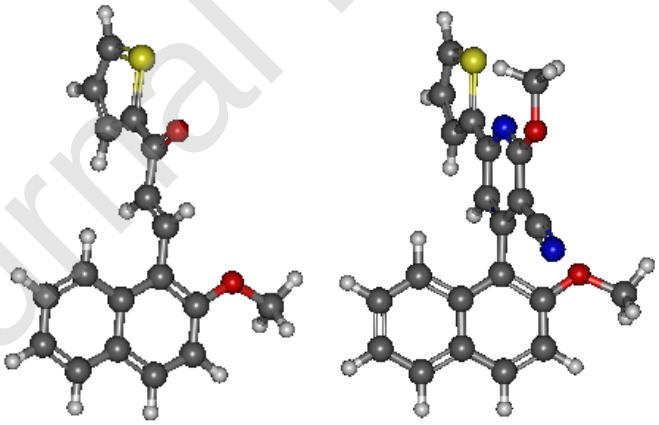

(a) **(b)**

Figure 10: First electronic excited state structure of (a) NC1 and (b) CP1 obtained using TD-B3LYP/6-311++G(d,p) level of theory.

The origin of this change in structure can be understood from the HOMO→LUMO transitions for first excited states of molecules under consideration. Figure 11(a)-(d) shows HOMO and LUMO for NC1

and CP1 molecules. As it is evident form Figure 11(a) and (b), in case of NC1, HOMO is a π orbital where electron density is localized on C=C bonds of naphthalene and linear chain. Excitation of an electron from HOMO(π) to LUMO(π*) changes the electron density to C-C bonds of linear chain. Such a strong shift of electron density can possibly change the intra-molecular interactions such as hyperconjugation and steric interactions leading to twist of the C=C bond to make the molecule non-planar in its first excited state. The molecule CP1 has more rigid frame compared to NC1, with pyridine ring directly connected to the naphthalene ring. In this molecule also, HOMO(π) shows the accumulation of electron density on C=C bands of naphthalene whereas LUMO(π*) shows the electron density on pyridine and thiophene rings. Although this also represents strong migration of electron density in HOMO→LUMO transition for the first excited state, the rigid molecular frame prevent the very large modulation in the structure, as it is seen in the case of NC1.

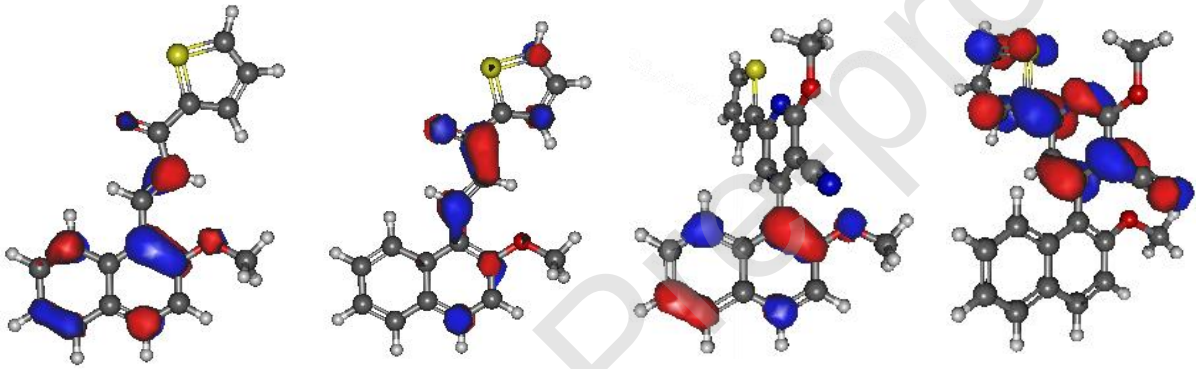

(a) NC1: HOMO (b) NC1: LUMO (c) CP1: HOMO (d) CP1: LUMO

Figure 11: HOMO and LUMO orbitals for molecules NC1 and CP1.

To obtain the UV-Vis absorption spectrum through DFT calculations, six lowest singlet excited states were calculated by using the vertical excitation from the ground state optimized geometry as shown in Figure 1(a) and (b). Various orbital interactions involved excited state 1 to excited state 6 for NC1 and CP1 are listed in supplementary Table S5 and S6. The corresponding orbitals are shown in supplementary Figure S7 and S8. The calculated UV-Vis spectrum of NC1 is shown in Figure 12. As it can be seen, for NC1, the first excited state is due to HOMO→LUMO transition, and it is the most prominent π→π* transition with oscillator strength 0.4253. The corresponding vertical absorption is at 402.56 nm. The second excited state has fifty times lower oscillator strength (0.0086) and corresponds to n→π* transition between HOMO-3→LUMO. The vertical absorption for excited state 3 to 6 in the

spectral region 295-325 nm are due to $\pi \rightarrow \pi^*$ transitions with moderate oscillator strength of 0.0615 – 0.0963.

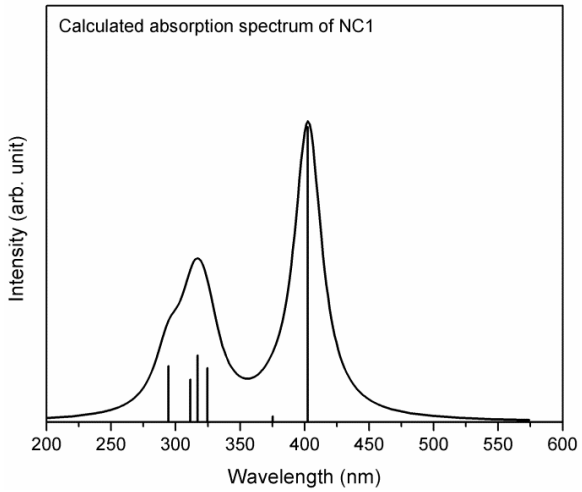

Figure 12: UV-Vis absorption spectrum of NC1. Six lowest singlet excited states are shown as stick and convolution.

The experimentally obtained UV-Vis spectrum of NC1 in DMSO is shown in Figure 13. As it is seen in the Figure 13, three prominent peaks appeared at 272, 324 and 356 nm. The band at 356 nm could be due to the first excited state. It is however lower by 52 nm relative to the calculated vertical excitation wavelength. It has to be noted that the calculations were made in gas phase. Moreover the structure of NC1 in first excited state obtained adiabatically shows a strong twisting of C-C bond. The observed shift in the first excited state could be due to structural modulation in the process of excitation.

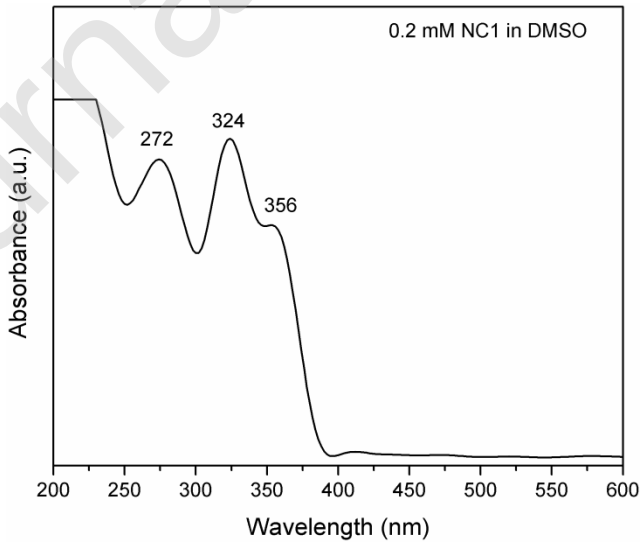

Figure 13: UV-Vis spectrum of NC1 obtained with 0.2mM concentration in DMSO. Strong absorption in 200-230 nm spectral range could be due to the solvent.

In usual condition, the adiabatically calculated energy for singlet excited state closely corresponds to the emission energy. The plot of adiabatic energy for the molecule NC1 in the first excited state is shown in Figure 14. This first excited state shows transition centered at 517.1 nm. The observed band in the fluorescence spectrum at 537 nm resembles very closely this calculated energy and thus the observed fluorescence spectrum is due to $\pi \rightarrow \pi^*$ transition between first excited state and ground state. The observed asymmetry in the fluorescence bands could be due to the emission from higher excited state.

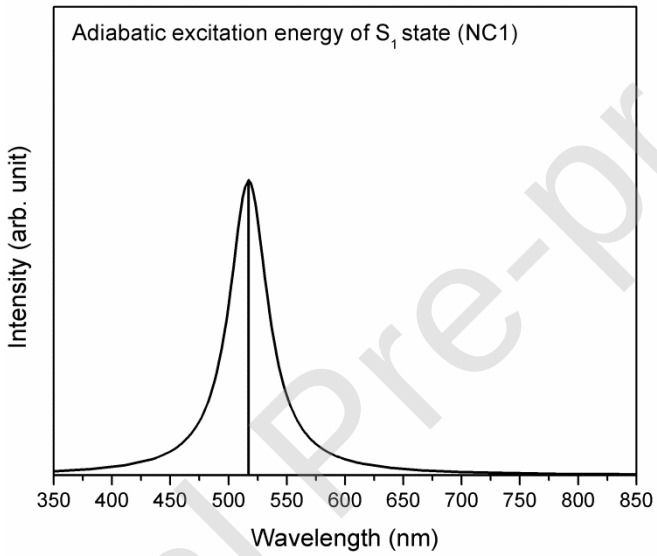

Figure 14: Emission spectrum of NC1 obtained from excitation of lowest excited state.

The calculated UV-Vis spectrum of CP1 is shown in Figure 15. In this molecule, the first excited state is HOMO→LUMO characterized as $\pi \rightarrow \pi^*$ at 399.4 nm with oscillator strength 0.0449. The second excited state is the most prominent feature at 336.8 nm in the calculated spectrum which is another $\pi \rightarrow \pi^*$ transition between HOMO-1→LUMO with oscillator strength 0.5641. Excited state 3-6 are also $\pi \rightarrow \pi^*$ with lower oscillator strength appears between 289-313 nm.

Experimental UV-Vis absorption spectrum of CP1 (0.1mM in DMSO) is shown in the Figure 16. The spectrum shows strong and broad absorption peak at 277 and 348 nm. The band at 348 nm possibly corresponding to the calculated second excited state and is of $\pi \rightarrow \pi^*$ characteristic. The less prominent band at 277 nm could be corresponding to calculated excited state 3-6.

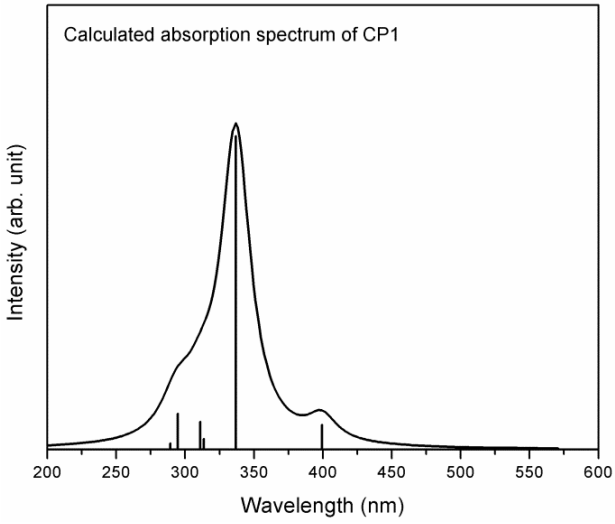

Figure 15: UV-Vis absorption spectrum of CP1. Six lowest singlet excited states are shown as stick and convolution.

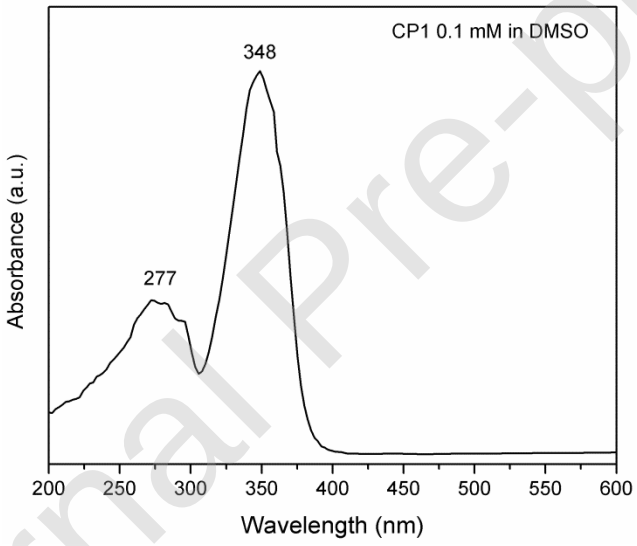

Figure 16: Emission spectrum of CP1 obtained from excitation of lowest excited state.

Figure 17 shows the adiabatic energy for the first excited state of CP1. In the adiabatic calculation of first excited state, the emission from the first excited state ($\pi \rightarrow \pi^*$) was found to be located at 501.08 nm showing the Stoke shift of ~113 nm. In the fluorescence spectrum a band at 530 nm is observed which possibly is due to emission from the first excited state and is of $\pi \rightarrow \pi^*$ nature. The 460 nm band observed in the fluorescence spectrum could be due to the emission from second excited state. The higher intensity of band at 460 nm is possibly due to higher absorption to second excited state as shown in Figure 15.

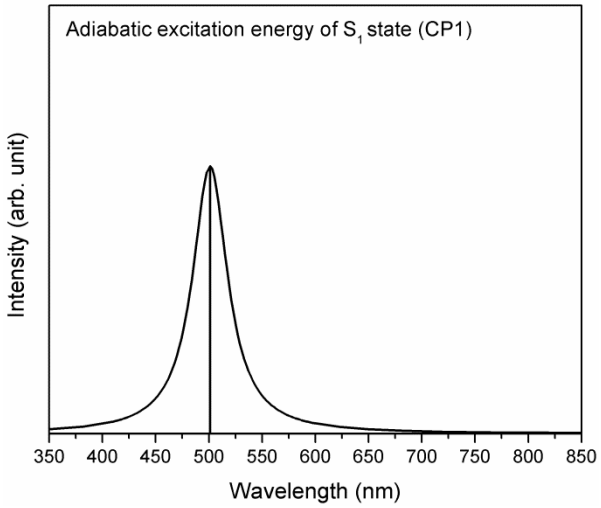

Figure 17: Emission spectrum of CP1 obtained from excitation of lowest excited state.

4. Conclusion:

The Claisen Schmidt condensation between acetyl thiophene and 2-methoxy-1-naphthaldehyde under basic condition followed by the heterocyclization can be used for the synthesis of targeted cyanopyridine derivatives in good yield. Resulted α, β-unsaturated ketone was heterocyclised to form cyanopyridines using malononitrile in the presence of sodium methoxide as a catalyst. Structures of the resulted compounds were established using FTIR, ^{1}H NMR and ^{13}C NMR studies. The photochemical behavior of the target molecules was investigated and have shown few interesting results. The chalcone (NC1) showed one major emission around 537 nm whereas the cyanopyridine derivative (CP1) has shown two emission bands at 460 and 530 nm in solution phase. The solid-state emission of chalcone derivative is observed in orange region which makes it suitable for the OLED application. The DFT calculation of cyanopyridine for the excited state revealed the change in the angle between naphthalene and pyridine plane which can ascertained for the HOMO to LUMO excitation. This property would make these molecules considerable for the optical materials.

References

1. J. R. Dimmock, D. W. Elias, M. A. Beazely, N. M. Kandepu, Bioactivities of chalcones, Curr. Med. Chem. 6 (1999) 1125-1149.

2. D. K. Mahapatra, S. K. Bharti, V. Asati, S. K Singh, Perspectives of medicinally privileged chalcone based metal coordination compounds for biomedical applications, Eur. J. Med. Chem. 174 (2019) 142-158.

3. V. Yerragunta, T. Kumaraswamy, D. Suman, V. Anusha, P. Prathima, T. Samhitha, A review on chalcones and its importance, Pharma Tutor 163 (2013) 54-59.

4. Sweety, S. Kumar, K. Nepali, S. Sapra, O. P. Suri, K. L. Dhar, G. S. Sarma A. K. Saxena, Synthesis and biological evaluation of chalcones having hetero substituent(s), Ind. J. Pharm. Sci. 72 (2010) 801–806.

5. S. L. Gaonkar, U. N. Vighnesh, Synthesis and pharmacological properties of chalcones: a review, Res. Chem. Intermed. 43 (2017) 6043–6077.

7. P. Singh, A. Anand, V. Kumar, Recent developments in biological activities of chalcones: a mini review, Eur. J. Med. Chem. 85 (2014) 758–777.

8. A. M. Asiri, S. A. Khan, Synthesis, characterization and optical properties of mono- and bis-chalcone,

Mater. Lett. 65 (2011) 1749–1752.

9. P. S. Patil, S. R. Maidur, S. V. Rao, S. M. Dharmaprakash, Growth and characterization of a new organic nonlinear optical crystal: 1-(3-nitrophenyl)-5-phenylpenta-2,4-dien-1-one, Opt. Laser Technol. 81 (2016) 70–76.

10. Z. K. Si, Q. Zhang, M. Z. Xue, Q. R. Sheng, Y. G. Liu, Novel UV-sensitive bis-chalcone derivatives: synthesis and photo-crosslinking properties in solution and solid PMMA film, Res. Chem. Intermed. 37 (2011) 635–646.

11. *(a)* R. Sens, K. H. Drexhage, Fluorescence quantum yield of oxazine and carbazine laser dyes**,** J. lumin. 709 (1981) 24-25; *(b)* Z. Xu, G. Bai, C. Dong, Spectral and photophysical properties of intramolecular charge transfer fluorescence probe: 4'-dimethylamino-2,5-dihydroxychalcone, Spectrochemica acta part A 62 (2005) 987-990; *(c)* Z. Xu, G. Bai, C. Dong, Studies on interaction of an intramolecular charge transfer fluorescence probe: 4′-Dimethylamino-2,5-dihydroxychalcone with DNA, Bioorg. Med. Chem. 13 (2005) 5694-5699; *(d)* C. G. Niu, A. L. Guan, G. M. Zeng, Y. G. Liu, Z.

W. Li. Fluorescence water sensor based on covalent immobilization of chalcone derivative, Analytica Chimica acta 577 (2006) 264-270; *(e)* T. A. Fayed, M. K. Awad, Dual emission of chalcone-analogue dyes emitting in the red region, Chem. Phys. 303 (2004) 317-326.

12. (*a*) E. D. D'Silva, D. Narayan Rao, R. Philip, R. J. Butcher, Rajnikant, S. M. Dharmaprakash, Synthesis, growth and characterization of novel second harmonic nonlinear chalcone crystal, J. Phys. Chem. Solids. 72 (2011) 824-830; (*b*) T. Chandra Shekhara Shetty, S. Raghavendra, C. S. Chidan Kumar, S. M. Dharmaprakash, Nonlinear absorption, optical limiting behavior and structural study of a new chalcone derivative-1-(3, 4-dimethylphenyl)-3-[4(methylsulfanyl) phenyl] prop-2-en-1-one, Opt. Laser Technol. 77 (2016) 23-30.

13. (*a*) E. Yang, C. Ruzie, M. Krayer, J. R. Diers, D. M. Niedzwiedzki, C. Kirmaier, J. S. Lindsey, D. F. Bocian, D. Holten, Photophysical properties and electronic structure of bacteriochlorin–chalcones with extended near- infrared absorption**,** Photochem. Photobiol. 89 (2013) 586-604; (*b*) K. G. Komarova, S. N. Sakipov, V. G. Plotnikov, M. V. Alfimov, Luminescent properties of chalcone and its amino derivatives**,** J. Lumin. 164 (2015) 57-63.

14. S. C. Lee, N. Y. Kang, S. J. Park, S. W. Yun, Y. Chandran, Y. T. Chang, Development of a fluorescent chalcone library and its application in the discovery of a mouse embryonic stem cell probe, Chem. Commun. 48 (2012) 6681–6683.

15. K. S. Parikh, R. P. Patel, Synthesis and characterization of some cyanopyridine compounds in therapeutic interest, Int. J. ChemTech Res. 1 (2009) 581-586.

16. W. J. Zhou; S. J. Ji; Z. L. Shen, An efficient synthesis of ferrocenyl substituted 3-cyanopyridine derivatives under ultrasound irradiation, J. Organomet. Chem. 691 (2006) 1356-1360.

17. V. R. Dangar, K. N. Borkhataria V. R. Shah, Synthesis, characterization and antimicrobial activity of cyanopyridine derivatives with Vanillin, Int. J. Pharm Sci. Res. 5 (2014) 20-24.

18. S. Liao, S. Shang, M. Shen, X. Rao, H. Si, J. Song, Z. Song, One-pot synthesis and antimicrobial evaluation of novel 3-cyanopyridine derivatives of (−)-β-pinene, Bioorg. Med. Chem. Lett. 26 (2016) 1512-1515.

19. F. F. Barsoum, Synthesis and vasodilation activity of some novel bis(3-pyridinecarbonitrile) derivatives, Eur. J. Med. Chem. 45 (2010) 5176-5182.

20. A. A. Amer, A. A. Abdelhamid, Microwave-assisted, one-pot multicomponent synthesis of some new cyanopyridines, J. Het. Chem. 54 (2017) 3126-3132.

21. M. A. EL-Hashash, S. S. Shaban, Synthesis and biological assessment of novel cyanopyridine derivatives, Synth. Comm. 49 (2019) 2073-2085.

22. O. Ostroverkhova, Organic optoelectronic materials: mechanisms and applications, Chem. Rev. 116 (2016) 13279−13412.

23. J. Zhao, J. I. Wong, C. Wang, J. Gao, V Z. N. Yun, H. Y. Yang, S. C. J. Loo, Q. Zhang, Synthesis, physical properties, and self-assembly of a novel asymmetric aroylene imidazo phenazine, Chem. Asian J. 8 (2013) 665 – 669.

24. T. N. Ahipa, V. Kumar, A. V. Adhikari, Synthesis, structural analysis and solvatochromic behaviour of 4, 6-bis (4-butoxyphenyl)-2-methoxynicotinonitrile mesogen, Liq. Cryst. 40 (2013) 31–38.

25. O. V. Ershov, M. Yu. Ievlev, M. Yu. Belikov, K. V. Lipin, A. I. Naydenova, V. A. Tafeenko Synthesis and solid-state fluorescence of aryl substituted 2-halogenocinchomeronic dinitriles, RSC Adv. 6 (2016) 82227-82232.

26. H. Zollinger, Color Chemistry, VHCA, Zurich, third ed, Switzerland, 2003.

27. H. Hegde, C. Ahn, D. Shwetha, S. L. Gaonkar, N. S. Shetty, Synthesis of new pyrazoline derivatives and its antimicrobial and antioxidant activities, J. Korean Chem. Soc. 61 (2017) 291-295.

28. M. W. Schmidt, K. K. Baldridge, J. A. Boatz, S. T. Elbert, M. S. Gordon, J. H. Jensen, S. Koseki, N. Matsunaga, K. A. Nguyen, S. Su, T. L.Windus, M. Dupuis, J. A. Montgomery, General atomic and molecular electronic structure system, J. Comput. Chem. 14 (1993) 1347-1363.

29. Y. Song, S. Zhu, S. Xiang, X. Zhao, J. Zhang, H. Zhang, Y. Fu, B. Yang, Investigation into the fluorescence quenching behaviors and applications of carbon dots, Nanoscale 6 (2014) 4676-4682.